

submitted to ApJ January 13, 2004

A Unified View of Coronagraph Image Masks

Marc J. Kushner¹

*Princeton University Observatory
Peyton Hall, Princeton, NJ 08544*

mkuchner@astro.princeton.edu

ABSTRACT

The last few years have seen a variety of new image mask designs for diffraction-limited coronagraphy. Could there still be useful designs as yet undiscovered? To begin to answer this question, I survey and unify the Fraunhofer theory of coronagraph image masks in the context of a one-dimensional classical coronagraph. I display a complete solution to the problem of removing on-axis light assuming an unapodized entrance aperture and I introduce the attenuation function, a measure of a generic coronagraph's off-axis performance. With these tools, I demonstrate that the masks proposed so far form a nearly complete library of image masks that are useful for detecting faint extrasolar planets.

Subject headings: astrobology — circumstellar matter — instrumentation: adaptive optics — planetary systems

1. INTRODUCTION

In a classical coronagraph (Lyot 1939), an image mask placed at a telescope's focus and a Lyot stop in a succeeding pupil plane block most of the light from a bright on-axis source allowing the telescope to better image faint off-axis sources. Classical coronagraphs have provided the first images of a brown dwarf orbiting a nearby star (Nakajima et al. 1995) and striking images of circumstellar disks (e.g. Smith & Terrile 1984; Clampin et al. 2003) and promise to enable imaging of bright extrasolar planets within the next decade (Trauger

¹Hubble Fellow

et al. 2003). Initial studies suggest that classical coronagraphs can potentially image even extrasolar terrestrial planets (see the review by Kuchner & Spergel 2003).

The last few years have seen a cornucopia of new coronagraph designs, including a variety of new image mask designs, typically invented using Fraunhofer diffraction theory. Perhaps construction tolerances and vector electromagnetic effects will limit the practicality of all these designs. However, the more choices of masks we have explored using Fraunhofer theory, the more likely it seems we may find a useful one for terrestrial planet finding. With extrasolar terrestrial planets in mind, I attempt to develop a unified picture of coronagraph image masks to determine the range of potentially useful solutions to the Fraunhofer diffracted-light problem. I concentrate first on a one-dimensional coronagraph with a tophat entrance aperture and then consider more general entrance apertures.

2. A SIMPLE CORONAGRAPH

We will examine a one-dimensional coronagraph (Sivaramakrishnan et al. 2001) comprising an entrance aperture, A , an image mask, \hat{M} , and a Lyot stop, L , each of which is represented by a complex-valued function constrained to have absolute value ≤ 1 . We use the notational conventions of Kuchner & Traub (2002) and Kuchner & Spergel (2003); letters with hats represent pupil plane quantities, and quantities transform as follows:

$$M(u) = \text{FT}[\hat{M}(x)] = \int_{-\infty}^{\infty} \hat{M}(x) e^{-2\pi i u x} dx. \quad (1)$$

We will assume the optics have removed any quadratic phase terms associated with small focal lengths. We will set all time-varying factors in the electric fields equal to 1; whenever we say “field”, we mean the amplitude of the time varying field. Mostly we will discuss monochromatic effects, though sometimes we will consider the effects of finite bandwidth.

We will use dimensionless units, but our units can be translated into physical distances as follows. In the pupil planes, our coordinates (u, u_1) measure distance from the optical axis in units of the local pupil diameter, which for example, at the primary mirror would simply be D , the diameter of the primary mirror. However, since the model is one dimensional, the primary mirror doesn’t have a diameter so much as a width; it extends forever in one direction. In the image planes, our coordinates $(x, \theta, \text{etc.})$ measure distance from the optical axis in units of the diffraction scale, which is ordinarily λf , where λ is the wavelength of light and f is the focal ratio. In the plane of the sky, they measure angle from the optical axis in units of λ/D radians.

An incoming wave incident on the entrance aperture creates a field with amplitude

$E(u)$. In our model, when an incoming wave interacts with a stop or mask, the function representing the mask multiplies the wave's complex amplitude. So after the wave interacts with the entrance aperture, the amplitude becomes $A(u) \cdot E(u)$.

After interacting with the entrance aperture, the beam propagates to an image plane, where the new field amplitude is the Fourier transform of the pupil plane field amplitude, $\hat{A}(x) * \hat{E}(x)$, where $*$ denotes convolution. There the beam interacts with the image mask, and the field amplitude becomes $\hat{M}(x) \cdot (\hat{A}(x) * \hat{E}(x))$. Then the beam propagates back to a second pupil plane, where the field amplitude is $M(u) * (A(u) \cdot E(u))$.

In the second pupil plane, the wave interacts with a Lyot stop, changing the field amplitude to $L(u) \cdot [M(u) * (A(u) \cdot E(u))]$. Then the beam propagates to a final image plane, where the final image is $\hat{L}(x) * [\hat{M}(x) \cdot (\hat{A}(x) * \hat{E}(x))]$. For a point source, the intensity of the final image is proportional to the absolute value of this quantity squared.

A coronagraph aims to reduce the final image of an on-axis point source, for which $E(u)$ is a constant, which we can set equal to 1. The field created by such a source in the second pupil plane, after the Lyot stop, is $L(u) \cdot (M * A)$ (Sivaramakrishnan et al. 2001). The corresponding final image field is the Fourier transform of this quantity, $\text{FT}(L \cdot (M * A))$. Masks for which

$$[L \cdot (M * A)](u) = 0 \quad (2)$$

will block identically all of the light from an on-axis point source; we aim to find these masks. This paper concerns solutions and approximate solutions to this linear problem.

2.1. Tophat Entrance Aperture, Arbitrary Lyot Stop

We will examine first a system where the entrance aperture, $A(u)$, is opaque ($A(u) = 0$) for $|u| > 1$ and transparent ($A(u) = 1$) for $|u| < 1/2$, and the Lyot stop, $L(u)$, is opaque for $|u| > (1 - \epsilon)/2$, where $\epsilon \leq 1$. To understand Equation 2 in the context of our simple coronagraph, we can write $A(u)$ as a difference of two Heaviside step functions, $H(u)$:

$$A(u) = H(u + 1/2) - H(u - 1/2) \quad (3)$$

Then, since convolution with a Heaviside step function represents indefinite integration, we can write

$$M(u) * A(u) = \mathcal{M}(u + 1/2) - \mathcal{M}(u - 1/2) \quad (4)$$

where $(d/du)\mathcal{M}(u) = M(u)$. Now we can see that Equation 2 demands only that

$$\mathcal{M}(u + 1/2) = \mathcal{M}(u - 1/2) \quad \text{for } -(1 - \epsilon)/2 < u < (1 - \epsilon)/2 \quad (5)$$

or equivalently.

$$\mathcal{M}(u) = \mathcal{M}(u - 1) \quad \text{for } \epsilon/2 < u < 1 - \epsilon/2. \quad (6)$$

An uncountable infinity of non-trivial masks meet this symmetry criterion. Figure 1a shows a generic function, $\mathcal{M}(u)$ that satisfies Equation 6. In the region $\epsilon/2 < u < 1 - \epsilon/2$, $\mathcal{M}(u)$ looks the same as it does in the region $-\epsilon/2 < u < -(1 - \epsilon/2)$; outside those regions, the function shown in Figure 1a has some random squiggles, to remind you that Equation 6 doesn’t specify anything about the function there.

2.2. Notch Filter Masks and Band-Limited Masks

Figure 1b shows the simplest interesting solution to Equation 6:

$$\mathcal{M}(u) \equiv \text{constant} \quad \text{for } \epsilon/2 < |u| < 1 - \epsilon/2. \quad (7)$$

This statement about $\mathcal{M}(u)$ translates into two requirements on $M(u)$:

$$M(u) = 0 \quad \text{for } \epsilon/2 < |u| < 1 - \epsilon/2 \quad (8)$$

and

$$\int_{-\epsilon/2}^{\epsilon/2} M(u) du = 0. \quad (9)$$

We can call functions $\hat{N}(x)$ whose Fourier transforms, $N(u)$, satisfy Equation 8 “notch filter” functions. Masks satisfying Equation 7 or equivalently, both Equations 8 and 9, are called notch filter masks (Kuchner & Spergel 2003; Debes et al. 2004).

Notch filter masks for which $M(u) = 0$ for $|u| > \epsilon/2$ are called band-limited masks (Kuchner & Traub 2002). Band-limited masks are an important subset of notch-filter masks because as we will see below, only the low-wavenumber components of any mask affect the off-axis light. Naturally, band-limited functions display wide variation, from the $\hat{M}(x) = \sin^2(\pi\epsilon x/2)$ mask that optimizes inner working angle, to masks where $\hat{M}(x)$ is a prolate spheroidal wavefunction (Kasdin et al. 2003). These latter masks optimize search area. The Gaussian mask (Sivaramakrishnan et al. 2001) is a good approximation to the prolate-spheroidal wavefunction band-limited mask.

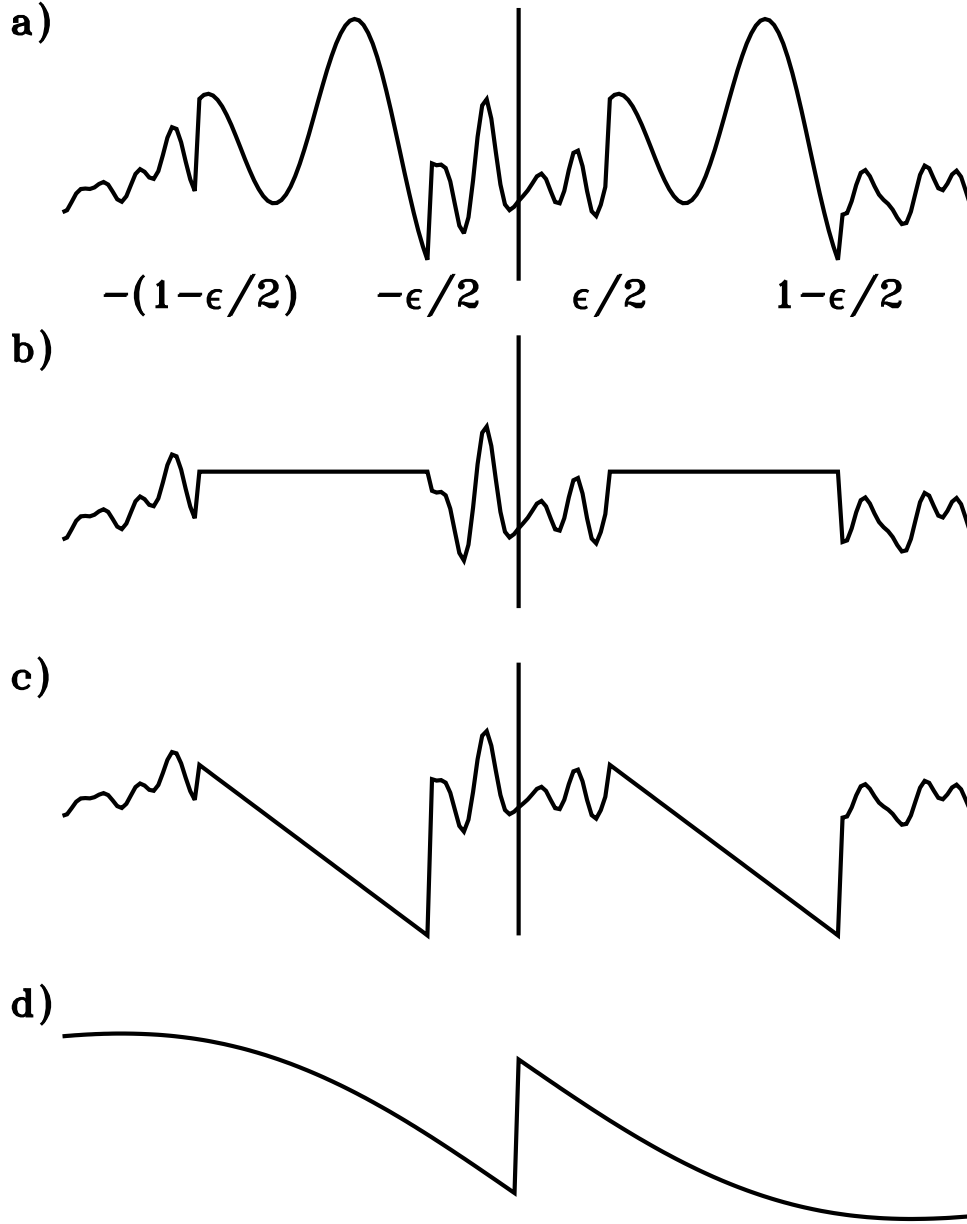


Fig. 1.— $\mathcal{M}(u)$ for a) a generic solution of Equation 6, b) a zeroth order, or notch filter mask c) a first order mask d) a 1-D disk phase mask, a good approximation to a first order mask. Eliminating on-axis light in a 1-D coronagraph with tophat entrance aperture requires finding a function with this translational symmetry.

2.3. First Order Masks

The next simplest solution to Equation 6 is one that adds a linear slope to $\mathcal{M}(u)$, while maintaining the needed translational symmetry. I.e.,

$$\mathcal{M}(u) \equiv \begin{cases} k_1 u & \text{for } \epsilon/2 < u < 1 - \epsilon/2 \\ k_1(u + 1) & \text{for } -(1 - \epsilon/2) < u < -\epsilon/2. \end{cases} \quad (10)$$

Figure 1c shows an example of such a sawtooth-like function. When $\mathcal{M}(u)$ takes this form,

$$M(u) = k_1 \quad \text{for } \epsilon/2 < |u| < 1 - \epsilon/2 \quad (11)$$

and

$$\int_{-\epsilon/2}^{\epsilon/2} M(u) du = -k_1(1 - \epsilon). \quad (12)$$

Equations 11 and 12 contain Equations 8 and 9 as a special case ($k_1 = 0$).

Mask functions $\hat{M}(x)$ that solve Equations 11 and 12 can always be decomposed into a sum of a notch-filter function and a δ -function. For example, a $1 - \delta$ -function mask

$$\hat{M}(x) = 1 - \delta(x) \quad (13)$$

$$M(u) = \delta(u) - 1 \quad (14)$$

$$\mathcal{M}(u) = H(u) - u \quad (15)$$

fills the bill. We can call notch filter masks “zeroth order” masks, and this $1 - \delta$ -function mask a “first order” mask.

Of course, we can not build this $1 - \delta$ -function mask. The closest we can come is to build a mask that is everywhere equally transparent, but that generates a phase shift of π in the center:

$$\hat{M}(x) = \begin{cases} 1 & \text{for } |x| > 1/4 \\ -1 & \text{for } |x| < 1/4. \end{cases} \quad (16)$$

$$M(u) = \delta(u) - \sin(\pi u/2)/(\pi u/2) \quad (17)$$

$$\mathcal{M}(u) \approx H(u) - u + \frac{\pi^2}{72}u^3 - \dots \quad (18)$$

Figure 1d shows $\mathcal{M}(u)$ for this mask—it approximates the sawtooth-like exact solution of Figure 1c. The disk phase mask of Roddier & Roddier (1997) is a two-dimensional version of this approximate solution.

2.4. The Rest of the Series

Equation 6 shows that over some interval, $\mathcal{M}(u)$, and therefore $M(u)$ are periodic functions, with period 1. We can expand such functions as a Fourier series:

$$P(u) = \sum_{j=0}^{\infty} A_j \sin 2\pi jx + B_j \cos 2\pi jx \quad (19)$$

where A_j and B_j are complex. This series satisfies Equation 6. However, this solution would completely specify the function over all x ; Equation 6 offers more freedom than that. We can express a complete solution as the sum of the above Fourier series and any notch filter function:

$$M(u) = N(u) + \sum_{j=1}^{\infty} A_j \cos 2\pi(j-1)x + B_j \sin 2\pi(j-1)x \quad (20)$$

$$\hat{M}(x) = \hat{N}(x) + \sum_{j=1}^{\infty} C_j \delta(x - (j-1)) + D_j \delta(x + (j-1)), \quad (21)$$

where $C_j = (A_j - iB_j)/2$ and $D_j = (A_j + iB_j)/2$, as long as

$$\int_{-\epsilon/2}^{\epsilon/2} M(u) du = \int_{\epsilon/2}^{1-\epsilon/2} M(u) du \quad (22)$$

$$= \epsilon A_j \operatorname{sinc} \pi(j-1)\epsilon. \quad (23)$$

In other words, all masks that completely remove on-axis light in a coronagraph with a tophat entrance aperture can be represented as the sum of a notch filter function and a series of δ -functions located at $x = \dots, -2, -1, 0, 1, 2, \dots$. So far, we have only considered masks with all A_j and B_j equal to 0, which we called zeroth order masks, or masks with only $A_1 \neq 0$, which we called first order masks (there is no B_1). We can refer to masks with A_j or $B_j \neq 0$, for $j > 1$ as “higher order” masks.

We can also consider the situation where the Lyot stop is bigger than the entrance aperture; $\epsilon < 0$. In this case, the solution to Equation 2 takes the form

$$M(u) = H(u) + \sum_{j=1}^{\infty} A_j \cos 2\pi jx + B_j \sin 2\pi jx \quad (24)$$

$$\hat{M}(x) = \hat{H}(x) + \sum_{j=1}^{\infty} C_j \delta(x - (j-1)) + D_j \delta(x + (j-1)), \quad (25)$$

where $\hat{H}(x)$ is a high-pass filter function, i.e. one where $H(u) = 0$ for $|u| < 1 - \epsilon$. High-pass filter functions do not have any effect on the image, however; the functional part of the mask

is the series of δ -functions. One example of a mask that works (approximately) for $\epsilon < 0$ is the 1-D disk phase mask illustrated above. It does not suddenly fail if ϵ becomes small or negative—though the approximation to a δ -function degrades towards the edges of the pupil plane.

Masks containing a row of δ -functions may not be buildable, but we could build approximate versions, like the disk phase mask, and we could build low-pass-filtered versions of some masks by convolving the mask function with $\text{sinc}(2\pi x)$ for example, (though constructing such masks could be tricky!).

However, all masks in this series except for notch filter masks and first order masks face the following complication in a broad-band system. In a real optical system, $M(x)$ necessarily changes with the wavelength of the light, λ ; for an intensity mask, $\hat{M}(x) \approx \hat{M}(x\lambda/\lambda_0)$, where λ_0 is the reference wavelength used for the purpose of defining the diffraction scale. Other, wavelength-dependent effects may appear, or be built into the mask, but this dilation is intrinsic to a classical coronagraph.

Consequently, $\mathcal{M}(u) \approx \mathcal{M}(u\lambda_0/\lambda)$. The notch-filter solution, for which $\mathcal{M}(u)$ is constant over a large range in u , can trivially be made to work over a large range in λ because of its dilation symmetry. However, all other solutions will only work at one wavelength, unless $M(x)$ explicitly changes as a function of wavelength in some special way other than simple dilation.

3. OFF-AXIS LIGHT AND A MORE GENERAL CORONAGRAPH

Now we will assess the impact of a coronagraph on an off-axis source, like an extrasolar planets located at angle θ from the optical axis in the plane of the sky. We can proceed in the context of a more general problem, where $A(u)$ and $L(u)$ can be any functions at all that we can Fourier transform.

3.1. The Attenuation Function: Inner Working Angle

A band-limited mask is what-you-see-is-what-you-get; a coronagraph with a band-limited mask attenuates the field from a distant source by a factor of $\hat{M}(\theta)$ and the Point Spread Function (PSF) in such a coronagraph does not depend on θ . (Kuchner & Traub 2002). But in general, the PSF in a coronagraph depends on θ , and clearly, the shapes of many image masks do not directly show how the mask attenuates off-axis sources. How can we understand in general what a coronagraph does to image of an astronomical source?

Kuchner & Traub (2002) showed that the high wavenumber components of the mask function, those with $|u| > 1 - \epsilon/2$, do not affect how the mask interacts with off-axis light. Consequently, for any mask, we can convolve $\hat{M}(x)$ with $\text{sinc}(2\pi(1 - \epsilon/2)x)$ and get the same effective mask. For a notch filter mask, this operation just means looking the band-limited part of the mask, which as we mentioned, is trivial to interpret. We will apply a similar idea here to reveal the workings of any image mask.

Consider a point source, providing a field $\delta(x - x_1)$ in the plane of the sky, and a harmonic mask function $M(u) = m \delta(u - u_1)$. The field after the entrance pupil is $A(u) \exp(-2\pi i u x_1)$, and the field in the first image plane is $\hat{A}(x - x_1)$. The field after the image mask is $m \exp(2\pi i u_1 x) \hat{A}(x - x_1)$. The field in the second pupil plane is $m A(u - u_1) \exp(-2\pi i (u - u_1) x_1)$. The field after the Lyot stop is $m L(u) A(u - u_1) \exp(-2\pi i (u - u_1) x_1)$. The final field is $m \exp(2\pi i u_1 x_1) \text{FT}[L(u) A(u - u_1)] \delta(x - x_1)$. In other words, the point source response of this particular special coronagraph is an intensity pattern $|m \text{FT}[L(u) A(u - u_1)]|^2$ centered at $x = x_1$.

We can evaluate the field amplitude at the center of the pattern simply by replacing the Fourier transform with $\int_{-\infty}^{\infty} du$. Then we see that the amplitude attenuation provided by this coronagraph at the center of the image of a point source is

$$\hat{F}(x_1) = m e^{2\pi i u_1 x_1} [L(u_1) * A(-u_1)] \quad \text{for a harmonic mask.} \quad (26)$$

The intensity at the center of the Point Spread Function (PSF) is $|\hat{F}(x_1)|^2$. We can call $\hat{F}(x_1)$ the coronagraph's amplitude attenuation function and $|\hat{F}(x_1)|^2$ the coronagraph's intensity attenuation function.

We can find the attenuation function for any arbitrary mask by expanding the mask function as $M(u) = \int_{-\infty}^{\infty} M(u_1) \delta(u - u_1) du$. Then the attenuation function becomes a Fourier integral:

$$\hat{F}(x_1) \equiv \int_{-\infty}^{\infty} M(u) e^{2\pi i u x_1} [L(u) * A(-u)] du \quad (27)$$

$$= \text{FT}(M \cdot (L(u) * A(-u)))(x_1) \quad (28)$$

$$= \left[\hat{M} * \left(\hat{L} \cdot \hat{A}^\dagger \right) \right] (x_1), \quad (29)$$

where \dagger denotes complex conjugation. This definition applies for any arbitrary entrance aperture, image mask, or Lyot stop. The PSF shape may change as a function of x_1 , the location of the off-axis source. However, the center of the PSF is usually the maximum of the PSF, so the attenuation function measures a critical feature of the mask for the purpose of finding off-axis point sources, like extrasolar planets.

Equation 29 shows that while a mask may look to us like it has sharp edges, in some sense it looks to the sky like it is smooth—convolved with a smoothing kernel of the form $\hat{L} \cdot \hat{A}^\dagger$. For example, the δ -function mask described above has an amplitude attenuation function $\hat{F}(x) = 1 - [\hat{L} \cdot \hat{A}^\dagger](x)$. If the Lyot stop is a tophat function and ϵ is small, then $\hat{F}(x) \approx 1 - \text{sinc}^2(\pi x/2)$. If the image mask is band-limited, then $\hat{F}(x_1) = \hat{M}(x_1)$.

Figure 2 shows how $\hat{F}(x)$ is constructed for a coronagraph with a tophat entrance aperture, tophat image mask, and tophat Lyot stop. The left column shows image plane quantities, and the right column shows their pupil plane conjugates. Figure 2a, b, and c show the entrance aperture, A , the image mask, \hat{M} , and the Lyot stop, L . Figure 2d shows the convolution of $L(u)$ and $A(u)$ and the image plane conjugate of this function, $\hat{L}(x)\hat{A}(x)$. These quantities act respectively as filter function and smoothing kernel. The amplitude attenuation function, $\hat{F}(x)$, shown in Figure 2e, is a smoothed version of the mask.

In this example, $L(u) * A(u)$ is a constant for $|u| < \epsilon/2$, and zero for $|u| > 1 - \epsilon/2$, as shown in Figure 2d. Consequently, if $M(u)$ were a band-limited mask function with power only where $|u| < \epsilon/2$, then multiplying $M(u)$ by $L(u) * A(u)$ would only serve to multiply $M(u)$ by a constant. In other words, $\hat{M}(x)$ would be an eigenfunction of convolution with $\hat{L}(x) \cdot \hat{A}(u)$.

Figure 3 shows $\hat{M}(x)$ and $\log |\hat{F}(x)|^2$ for several different image masks: a phase knife (Equation 31), a tophat mask, a one-dimensional disk phase mask (Equation 17), a Gaussian mask, and a band-limited mask ($\hat{M}(x) = 1 - \text{sinc}^2(\pi \epsilon x/2)$). Of the masks shown, only the phase knife and the band-limited mask provide $\hat{F}(0) = 0$. Of those, only the band-limited mask provides perfect cancellation of on-axis light and the deep null needed for terrestrial planet finding.

The attenuation function provides a good metric for the inner working angle, θ_{IW} of a coronagraph. For example, we could define the inner working angle by $|\hat{F}(\theta_{IW})|^2 = 1/2$. With this definition, and assuming a tophat Lyot stop with $\epsilon = 0$, $\theta_{IW} = 0.58\lambda/D$ for the δ -function image mask, and $0.43\lambda/D$ for a phase knife. For comparison, the smallest possible inner working angle for a band-limited mask is $\theta_{IW} = 0.64\lambda/D$ —except that for this band-limited mask, $\epsilon = 1$, so the coronagraph would have no throughput.

Notice that with a mask that is not a notch filter mask, apodizing the Lyot stop makes \hat{L} into a broader function, which increases the coronagraph’s inner working angle. Likewise, we could push the inner working angle inwards if we replaced the Lyot stop with a pair of pinholes at $u = \pm 1/2$, for example. However, in reality, these distinctions probably don’t matter, because low order aberrations, like pointing error, will probably set the inner working angle of a real coronagraph

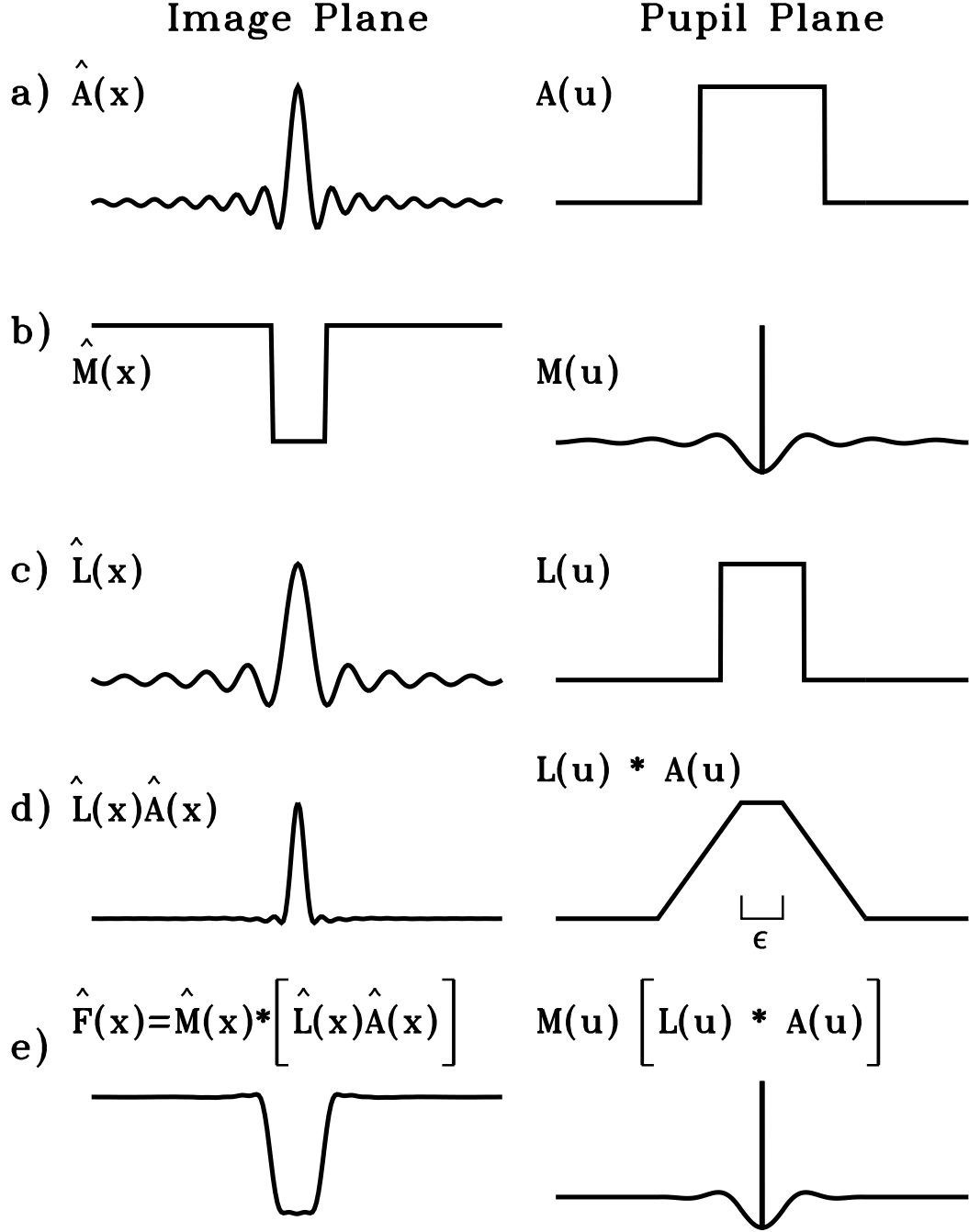


Fig. 2.— Constructing the attenuation function, a smoothed version of the mask that the planets see. a) entrance pupil and its Fourier conjugate b) image mask and its conjugate c) Lyot stop and its conjugate d) the smoothing kernel and the filter function e) the amplitude attenuation function, $\hat{F}(x)$, and its conjugate.

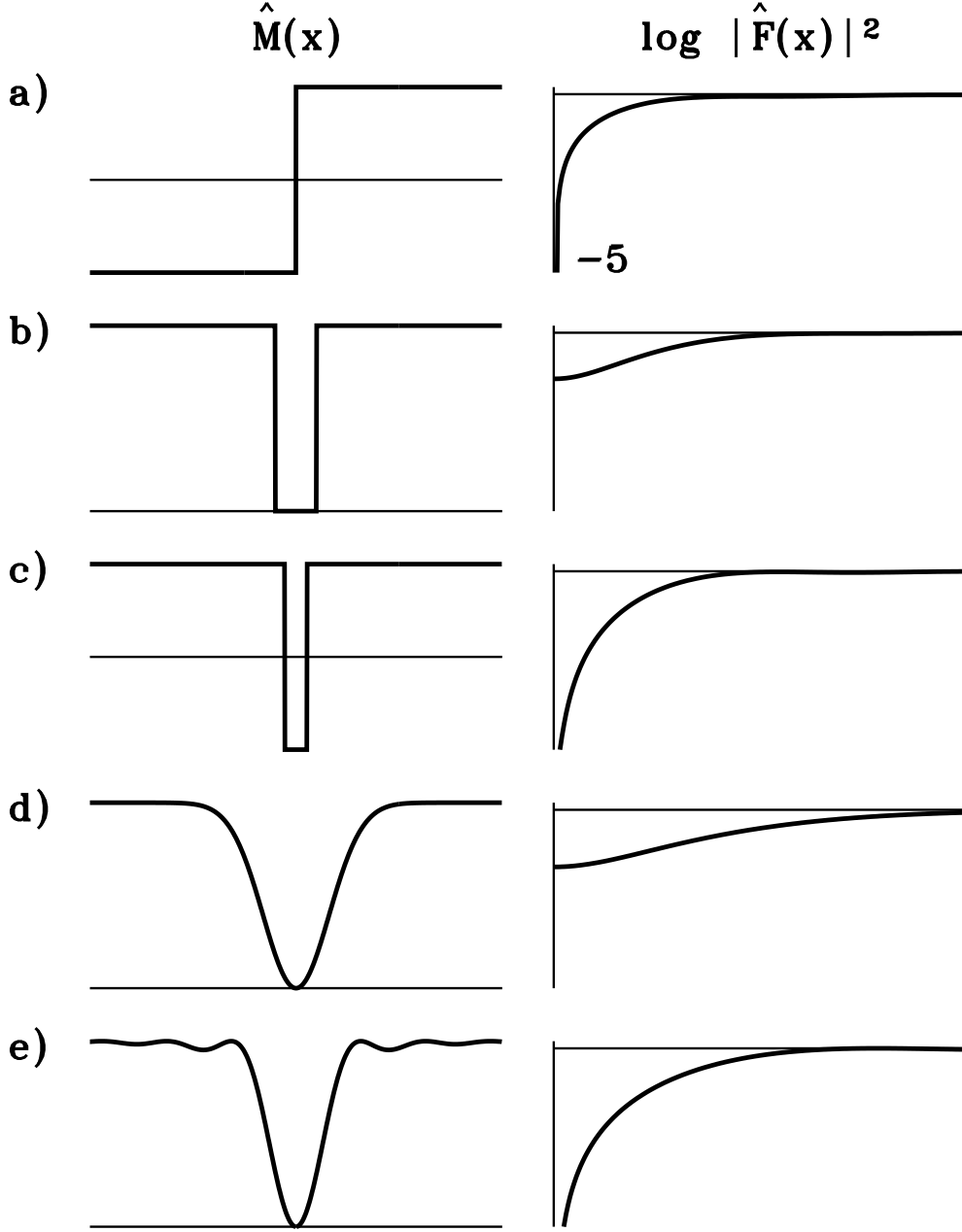


Fig. 3.— Mask functions, $\hat{M}(x)$, and intensity attenuation functions, $|\hat{F}(x)|^2$, for several image masks, calculated assuming the entrance aperture and Lyot stop are identical tophat functions. a) Phase Knife b) Tophat c) 1-D Phase Disk d) Gaussian e) $1 - \text{sinc}^2$ (Band-Limited)

3.2. Mask Symmetry and Stellar Leak

By taking derivatives of Equation 29, we can construct a Taylor expansion for $\hat{F}(x)$ about $x = 0$:

$$\hat{F}(x) = \sum_n \frac{x^n}{n!} \int_{-\infty}^{\infty} M(u) (2\pi i u x_1)^n [L(u) * A(-u)] du. \quad (30)$$

Consider a system where $L(u)$ and $A(u)$ have even symmetry. If $M(u)$ has even symmetry then $\left(\frac{d}{dx}\right)^n \hat{F}(x) \Big|_{x=0}$ will vanish for all odd n . If $M(u)$ has odd symmetry then $\left(\frac{d}{dx}\right)^n \hat{F}(x) \Big|_{x=0}$ will vanish for all even n . For example, in a coronagraph where $\hat{A}(x)$ and $\hat{L}(x)$ have even symmetry, if we use any image mask with odd symmetry, the on-axis final image field from an on-axis point source will be zero.

Mask functions, $\hat{M}(x)$, with odd symmetry necessarily become negative, so they require manipulating the phase of the beam. The simplest such mask is the phase-knife coronagraph (Abe et al. 2001), for which

$$\hat{M}(x) = \begin{cases} 1 & \text{for } x > 0 \\ 0 & \text{for } x = 0 \\ -1 & \text{for } x < 0. \end{cases} \quad (31)$$

A phase knife consists of a half-plane of glass joined to a half-plane of phase-retarding material so that the seam falls on the optical axis. We may be able to make a more practical version of this mask by laying an opaque strip over the seam so that the mask function becomes

$$\hat{M}(x) = \begin{cases} 1 & \text{for } x > s \\ 0 & \text{for } |x| < s \\ -1 & \text{for } x < -s. \end{cases} \quad (32)$$

where s is one or two diffraction widths. This variation retains the mask's odd symmetry, but removes the seams from direct illumination.

Though $\hat{F}(x=0) = 0$ for the phase knife, the mask does not eliminate all on-axis light. The on-axis source may produce an image with zero central intensity, but with bright wings that can overwhelm the image of an off-axis planet. A perpendicular pair of phase knives, like the four-quadrant phase mask (Rouan et al. 2000; Riaud et al. 2001, 2003; Lloyd et al. 2003) does a better job than a single phase knife at reducing these wings at the cost of some search area and also exactly satisfies Equation 2 for a circular entrance aperture and circular Lyot stop.

However, the wings of the image of an on-axis point source are not the only drawback to the phase-knife mask. Real stars do not provide perfect on-axis point sources; stars have

Table 1: Null Depth

Mask	Intensity Leak On Axis	Pointing Requirement (fraction of θ_{IW})
Tophat	θ^0	-
Disk Phase Mask	θ^0	-
Phase Knife	θ^2	0.0001
Four-Quadrant Phase Mask	θ^2	0.0001
All Masks With Odd Symmetry	θ^2	0.0001
Notch Filter	θ^4	0.01
Band-limited	θ^4	0.01
Gaussian	θ^4	0.01^a
Achromatic Dual Zone	θ^4	0.01^a

^aAssuming appropriate pupil stops that the zeroth order leak is negligible.

finite angular size and telescopes can not point at them perfectly accurately (e.g. Riaud et al. 2001; Kuchner & Traub 2002; Kuchner & Spergel 2003; Lloyd et al. 2003). We must consider the intensity leak from slightly off-axis starlight, which we can approximate by $|\hat{F}(\theta)|^2$, where θ is the angle off axis.

A common misconception is that disk phase masks are especially sensitive to pointing error. However, any coronagraph has a pointing error tolerance related to its inner working angle; the smaller the inner working angle, the tighter the tolerance. Disk phase masks have small inner working angles, so they have tight pointing tolerances. But at a given inner working angle, disk phase masks perform well.

In general, the leak increases as some power of θ . Equation 30 shows that the intensity leak from a mask with odd symmetry, like a phase-knife mask, is $\mathcal{O}(\theta^2)$. A notch filter mask has even symmetry, so the intensity leak from a notch-filter mask is $\mathcal{O}(\theta^4)$. The circular phase mask (Roddier & Roddier 1997) and the Gaussian mask have $F(x=0) \neq 0$, so they leak at $\mathcal{O}(\theta^0)$, though the zeroth order leak can be made negligible. All masks of containing sin terms in Equation 21 produce an $\mathcal{O}(\theta^2)$ intensity leak.

Viewed at quadrature, reflected visible light from the Earth is 2×10^{-10} times as bright as direct light the Sun. We do not need to suppress the starlight to quite this level in the center of the image plane since the planet appears typically a few diffraction widths from the star in the wings of the stellar leakage, which we can control with an apodized Lyot stop if necessary. A reasonable assumption might be that for terrestrial planet finding, we can

tolerate up to $\hat{F}(\Delta\theta) = 10^{-8}$, where $\Delta\theta$ is the effective pointing error (which may contain some contribution from the star’s finite angular size).

Given this assumption, we must center the star on the mask to an accuracy of roughly $\Delta\theta = 10^{-8/\beta}\theta_{IW}$, where the mask’s leak is $\mathcal{O}(\theta^\beta)$, and θ_{IW} is the coronagraph’s inner working angle. For example, a fourth-order intensity leak, or a fourth-order “null”, to use the language of interferometry, translates into a pointing requirement of $\Delta\theta \lesssim \theta_{IW}/100$. Table 1 summarizes the leading order intensity leaks from the masks discussed in this paper.

3.3. Other Directions: Apodized Entrance Apertures

We found a complete solution to the problem of removing on-axis light in a one-dimensional coronagraph with an un-apodized entrance aperture. However, several coronagraph designs, classical and otherwise, use apodized entrance pupils (Kasdin et al. 2003) or specially shaped pupils (Spergel 2001; Kasdin et al. 2003; Vanderbei et al. 2003a,b). Other designs use a pair of shaped mirrors to generate an apodized beam (Guyon 2003; Traub & Vanderbei 2003). These designs aim to suppress the wings of the PSF so far that the edges of the image mask are not illuminated by the image of an on-axis source, so a simple tophat mask suffices to remove the on-axis light to the necessary level. Achieving this suppression generally requires numerical optimization to find an approximate solution to Equation 2. Coronagraphs with apodized entrance apertures, like coronagraphs with apodized Lyot stops, are especially robust to low-order aberrations.

We can also find new exact solutions to Equation 2 using an apodized entrance aperture and a phase mask (Aime et al. 2002; Soummer et al. 2003). However, these exact solutions require $\hat{M}(x)$ to vary in a complicated way with wavelength. One design that provides a self-adjusting $\hat{M}(x, \lambda)$ to be combined with an apodized entrance aperture is the achromatic dual-zone phase coronagraph (Soummer et al. 2003). Achromatic dual-zone phase masks can be designed with $\mathcal{O}(\theta^4)$ leak. Combining image masks and apodized entrance pupils remains relatively unexplored territory—though perhaps such designs should not be called classical coronagraphs.

4. CONCLUSION

According to Fraunhofer diffraction theory, uncountably many non-trivial image mask designs can completely remove the light from an on-axis source in a classical coronagraph with an un-apodized entrance aperture. We organize these designs using a trigonometric

series solution to the equation $L \cdot (M * A) = 0$. Notch filter masks are the zeroth order solutions, and the only solutions that are trivially achromatic in our approximation over a large bandwidth. Higher order solutions can be decomposed into the sum of a notch filter function and a series of $\delta(x)$ functions; the disk phase mask (Roddier & Roddier 1997) approximates one term in the sum.

We defined the mask amplitude attenuation function, $\hat{F}(x)$, as the amplitude at center of the final image of a point source located at angle x off-axis in the plane of the sky. This function, which we showed is a smoothed version of the mask function, provides an easy way to judge the null depth and inner working angle for non-band-limited masks. Through this analysis, we showed that only masks with even symmetry can provide the null depth necessary for terrestrial planet searches; for example, masks based on a phase knife do not provide the necessary null depth.

We focused on a one-dimensional coronagraph with an un-apodized entrance aperture, though other designs may prove useful. For example, the full two-dimensional problem may yield surprises. Some coronagraph designs use apodized entrance pupils—though classical coronagraphs with apodized entrance pupils generally require $\hat{M}(x)$ to vary with wavelength in a complicated way. It may also be possible to gain benefit by cascading multiple image plane masks. But neglecting these avenues, our analysis shows that our existing library of one-dimensional image mask designs is complete.

Thanks to David Spergel, Wes Traub, and Ann Bragg for comments on this manuscript, and the folks at the Leiden Coronagraphy Workshop for inspiration. M.J.K. acknowledges the support of the Hubble Fellowship Program of the Space Telescope Science Institute.

REFERENCES

- Abe, L., Vakili, F. & Boccaletti, A. 2001, *A&A*, 374, 1161
- Aime, C., Soummer, R. & Ferrari, A. 2002, *A&A*, 389, 334
- Clampin, M. et al. 2003, *AJ*, 126, 385
- Debes, J., Ge, J., Kuchner, M. & Rogosky, M. 2004, submitted to *ApJ*
- Guyon, O. 2003, *A&A*, 404, 379
- Kasdin, N. J., Vanderbei, R. J., Spergel, D. N., & Littman, M. G. 2003, */apj*, 582, 1147

- Kasdin, J. K. 2004, The prolate spheroidal wavefunction mask paper.
- Kuchner, M. J. & Spergel, D. N. 2003, in *Scientific Frontiers in Research on Extrasolar Planets*, ASP Conference Series, D. Deming & S. Seager, eds.
- Kuchner, M. J. & Spergel, D. N. 2003, *ApJ*, 594, 617
- Kuchner, M. J. & Traub, W. A. 2002, *ApJ*, 570, 900
- Lloyd, J. P., Gavel, D. T., Graham, J. R., Hodge, P. E., Sivaramakrishnan, A. & Voit, G. M. 2003, *Proc. SPIE*, 4860, 171
- Lyot, B. 1939, *MNRAS*, 99,
- Nakajima, T. et al. 1995, *Nature*, 378, 463
- Riaud, P.; Boccaletti, A.; Baudrand, J.; Rouan, D. 2003, */pasp*, 115, 712
- Riaud, P., Boccaletti, A., Rouan, D., Lemarquis, F., & Labeyrie, A. 2001, */pasp*, 113, 1145
- Roddier, F. & Roddier, C. 1997, *PASP*, 109, 815
- Rouan, D., Riaud, P., Boccaletti, A., Cl  net, Y., & Labeyrie, A. 2000, *PASP*, 112, 1479
- Sivaramakrishnan, A., Koresko, C. D., Makidon, R. B., Berkefeld, T., & Kuchner, M. J. 2001, *ApJ*, 552, 397
- Smith, B. A. & Terrile, R. J. 1984, *Science*, 226, 1421
- Soummer, R., Aime, C. & Falloon, P. E. 2003, *A&A*, 397, 1161
- Soummer, R., Dohlen, K. & Aime, C. 2003, *A&A*, 403, 369
- Spergel, D. N. 2001, preprint (astro-ph/0101142)
- Traub, W. A., Vanderbei, R. J. 2003, *ApJ*, 599, 695
- Trauger, J. T. et al. 2003, *Proc. SPIE*, 4854, 116
- Vanderbei, R. J., Spergel, D. N., & Kasdin, N. J., 2003, *ApJ*, 590, 593
- Vanderbei, R. J., Spergel, D. N., & Kasdin, N. J. 2003, *ApJ*, 599, 686